9

Active Power Filters for Harmonic Elimination and Power Quality Improvement

António Martins[1], José Ferreira[2] and Helder Azevedo[3]
[1]*University of Porto,*
[2]*Metro do Porto, S.A.,*
[3]*Efacec - Engenharia e Sistemas, S.A.*
Portugal

1. Introduction

The explosive growth in consumer electronics and domestic appliances has generated a major concern in the electricity supply industry, (Bollen, 1999). Due to its interface circuit (a diode bridge, followed by a large DC capacitor), these appliances draw current only near the peak of the mains voltage. Like this circuit other power electronics based applications draw non-sinusoidal currents, despite the applied voltage being sinusoidal. Due to the non-ideal characteristics of the voltage source, harmonic currents create voltage distortion.
Non-linear loads such as rectifiers, cycloconverters, variable speed drives and arc furnaces, large decaying DC components, asymmetrical loads and other electrical equipment can cause high disturbances in the power supply system, (Bollen, 1999).
The harmonics generated by the most common non-linear loads have the following properties:

- lower order harmonics tend to dominate in amplitude;
- if the waveform has half-wave symmetry there are no even harmonics;
- harmonic emissions from a large number of non-linear loads of the same type will be added.

The major problems caused by the mains harmonic currents are those associated with the harmonic currents themselves, and those caused by the voltage waveform distortion resulting from the harmonic currents flowing in the supply source impedance. This distortion of the voltage waveform can cause, e.g. serious effects in direct on-line induction motors, ranging from a minor increase in internal temperature through excessive noise and vibration to actual damage; electronic power supplies may fail to operate adequately; increased earth leakage current through EMI filter capacitors due to their lower reactance at the harmonic frequencies.
To minimize these effects in electricity distribution systems (non-sinusoidal voltages, harmonic currents, unbalanced conditions, power de-rating, etc) different types of compensators have been proposed to increase the electric system quality, (Bollen, 1999, Hingorani & Gyugyi, 1999). One of those compensators is the active power filter (APF), (Akagi et al., 1984).
This Chapter is organized as follows: in Section 2, it is presented a brief review of power quality and harmonic emission standards, while Section 3 addresses main active filter

topologies, control methods and performance indexes. In Section 4 it is developed a prototype of an APF for demonstration purposes, including the operating principle of the current controlled filter, and Section 5 includes the design of the filter's passive elements. Simulation and experimental results in different operating conditions are presented in Section 6, including performance evaluation. Finally, Section 7 discusses conclusions related to the presented work and indicates some future research needed in this area.

2. Power quality and harmonic emissions standards

With the increased use of electrical and electronic equipment, and telecommunication and broadcasting transmissions the electromagnetic spectrum is becoming saturated. The equipment within residential, commercial or industrial installations has become increasingly sensitive to some type of electromagnetic interference (EMI) both from internal or external sources, primarily because of the use of digital technology. So there is a need for control of electromagnetic environment, namely by limiting of the harmonic emissions caused by any type of electrical or electronic equipment. In the European Union, this problem has been addressed by the Directive 2004/108/EC - the Electromagnetic Compatibility Directive; in the United States the main guideline comes from the IEEE Standard 519.

The EMC Directive incorporates standards mainly from the CISPR, the CENELEC, and the IEC organizations. The standards assist in achieving adequate power quality and in controlling it. They provide a framework within which the electricity distribution network environments, the susceptibility of equipment to low voltage quality, and the emissions from different types of equipment are all defined. Examples of standards relating to power quality characteristics and measurements are the EN 50160, the IEC 61000-4-30 and the IEEE Standard 1159.

The purpose of the EN 50160 standard is to specify the characteristics of the supply voltage with regard to the course of the curve, the voltage level, the frequency and symmetry of the three-phase network at the interconnecting point to the customer. The goal is to determine limiting values for regular operating conditions. However, facility defects may lead to major disturbances in the electricity distribution supply network. The complete breakdown of the network can no longer be described efficiently by limiting values. Thus there is no point in indicating actual limiting values. Accordingly, the standard establishes just these values as limiting values, which are not allowed to be exceeded or remained under during 95% of the controlled period. Rather than being an EMC standard the EN 50160 is a product standard giving the voltage characteristics which can be expected at the supply terminals. The EN 50160 standard is becoming a kind of reference for what should be seen as good power quality.

Like the EN 50160, the IEC 61000-4-30 and the IEEE 1159 are the first standards that define the characteristics of voltage waveform as obtained from measurements. The power quality parameters considered are grid frequency, magnitude of the supply voltage, flicker, supply voltage dips and swells, voltage interruptions, transients over voltages, supply voltage unbalance, voltage and current harmonics, voltage inter-harmonics and mains signalling on the supply voltage and rapid voltage changes. Depending on the purpose of the measurement, all of the phenomena on this list may be measured, or a subset of the phenomena on this list may be measured.

It is in this scenario of voltage/power quality issues related to the grid connection of electric/electronic loads or sources that the APF is an important player.

3. APF control methods and performance

3.1 APF topologies

In some industrial and commercial applications, electric power is distributed through three-phase four-wire systems. With incorrectly distributed or uncompensated loads such systems may suffer from excessive neutral currents caused by non-linear or unbalanced loads. In such conditions, a three-phase four-wire active filter can provide harmonic neutralisation, (Aredes et al., 1997, Montero et al., 2007). The main converter topologies for three-phase four-wire active power filters are the conventional three-leg converter with neutral point connection in the DC bus and the four-leg converter; the fundamental difference between them is the number of power semiconductor devices. In some conditions, even in three-phase installations, single-phase compensation can be advantageous. In such cases, the single-phase shunt active filter is often used, (Komurcugil & Kruker, 2006).
However, three-phase systems without neutral conductor are more general and will be the object of the present work.

3.2 Control methods and strategies

Different approaches such as notch filter, (Newman et al., 2002), scalar control, (Chandra et al., 2000), instantaneous reactive power theory, (Furuhashi et al., 1990, Akagi et al., 2007), synchronous detection method, (Chen et al., 1993), synchronous d–q frame method, (Mendalek et al., 2003), flux-based control, (Bhattacharya et al., 1996), and closed loop PI, (Bhattacharya et al., 1996), internal model control, (Marconi et al., 2007), and sliding mode control, (Saetieo et al., 1995), can be used to improve the active filter performance. Also, the direct power control method has found application in active filters, (Chen & Joós, 2008). Specific harmonics can be cancelled out in the grid using the selective harmonic elimination method (Lascu et al., 2007). In all cases, the goal is to design a simple but robust control system for the filter.
Usually, the voltage-source is preferred over the current-source to implement the parallel active power filter since it has some advantages, (Routimo et al., 2007). Using higher voltages in the DC bus is desirable and can be achieved with a multilevel inverter (Lin & Yang, 2004). In this Chapter it is used the voltage-source parallel topology, schematically shown in Fig. 1.

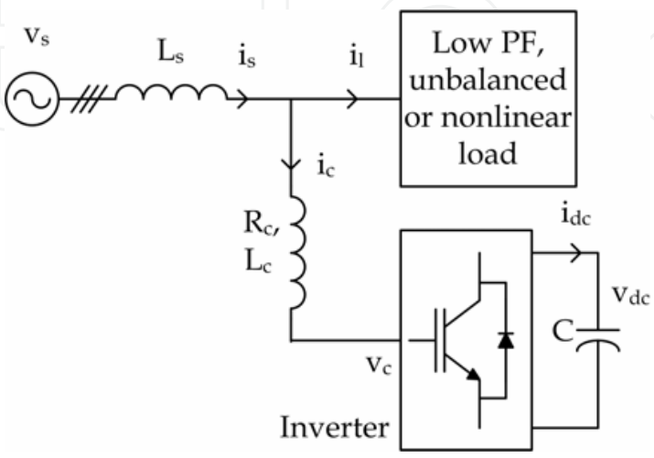

Fig. 1. Connection diagram of a voltage source active power filter.

The filter generates currents in the connection point in order to: 1- cancel/minimize the harmonic content in the AC system, 2- correct the power factor at fundamental frequency, 3- regulate the voltage magnitude, and 4- balance loads. So, the AC distribution system only carries the active fundamental component of the load current.

Very different current control algorithms can be applied to the active filter, (Akagi, 2005). The current reference for the active filter connection node usually satisfies one of the two following strategies: 1- power factor correction, harmonic elimination, and load unbalance compensation or, 2- voltage regulation, harmonic elimination, and load unbalance compensation.

The voltage regulation strategy is a concurrent objective faced to the power factor compensation because the two depend on the reactive current. However, any control algorithm has enough flexibility to be configured, in real-time, to either objectives or for the two, in a weighted form.

Even under the same compensation strategy, the filter can be controlled with different control algorithms. Two main approaches are common: voltage control, and current control. Both methods have advantages and weaknesses. In Fig. 2 it is represented a block diagram, with the variables shown in Fig. 1, of a voltage-based control algorithm of an active power filter implementing vector control.

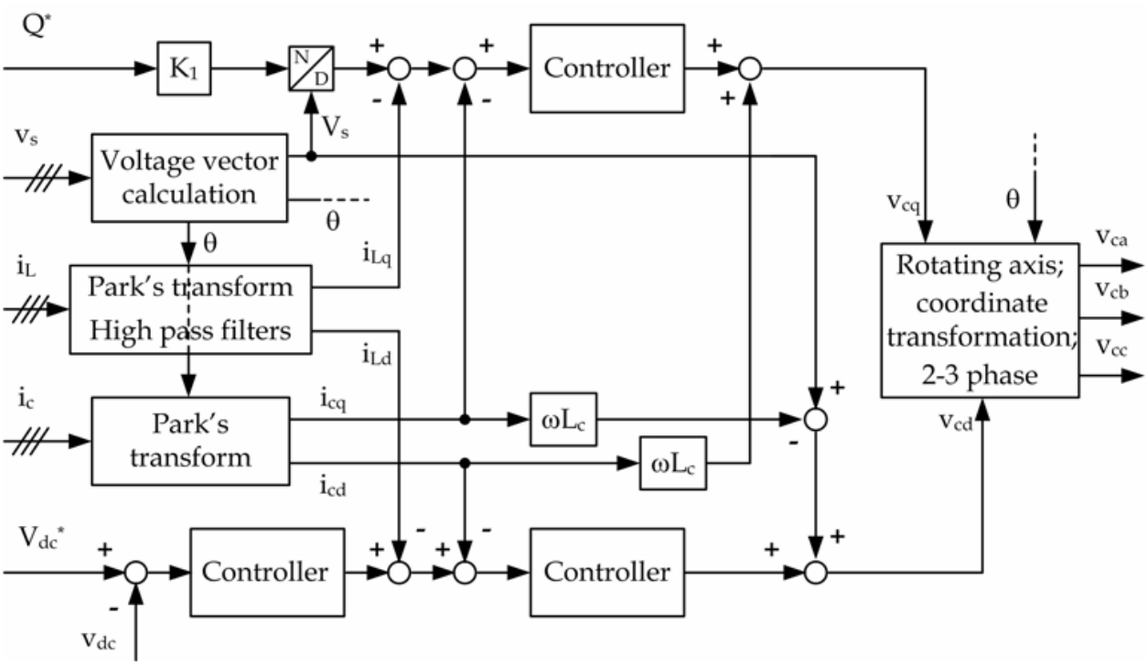

Fig. 2. Voltage control of the active power filter.

In the presence of the power quality concern the mains current is the most important variable to be controlled. This method indirectly controls the mains current through the filter output voltage.

In Fig. 3 it is shown a block diagram of a current-based control algorithm of an active power filter also capable of implementing different compensation strategies. This control method directly controls the mains current through the i_{sRef} signals. However, it has slower dynamics than the voltage-based method (Chandra et al., 2000).

A static power converter, like the one shown in Fig. 1, capable of doing (almost) all the above referred functions is necessarily very complex. This complexity arises from the following considerations:

- the converter dynamic behaviour must be very fast in order to be capable of compensate currents in a large spectra,
- the control algorithm must deal with a large number of variables such as mains voltages and currents, load currents, DC voltage and current, and
- high dynamic performance and better active and reactive power decoupling can demand direct and inverse coordinate transformation and a large amount of signal processing.

So, fast power electronics semiconductors, with high switching frequencies, and powerful control platforms are needed to build this type of power electronics systems.

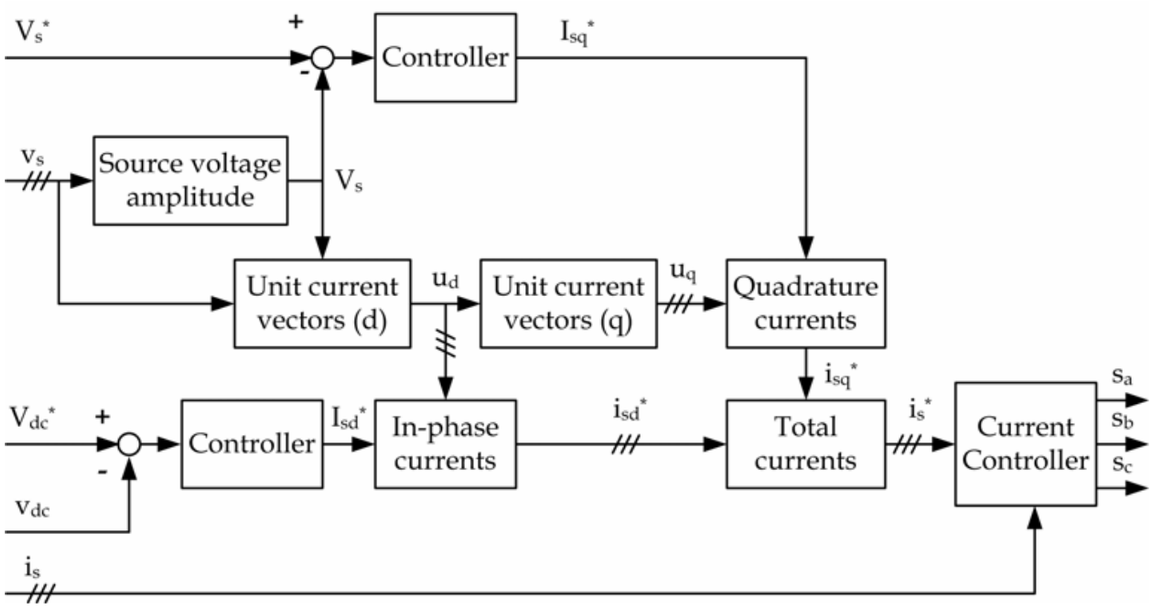

Fig. 3. Current control of the active power filter.

3.3 Performance evaluation of APFs

In order to analyze and evaluate the performance of an active power filter, different aspects must be considered. Two different performance types can be considered: the qualitative ones and the quantitative measures.

Qualitative evaluation

The qualitative value of an active power filter is a consequence of different technical merits. The most important ones are briefly described:

- power semiconductor characteristics, namely of diodes, GTOs and IGBTs, and converter topology,
- type of control system, scalar or vector control, and operating modes,
- converter supervision, diagnostics and remote control.

The active filter must accomplish one, or more than one, specific objective. So, its working conditions must be in agreement with the established purposes: reactive power

compensation; voltage regulation; load balancing or harmonic compensation. These operating modes should be programmable, remotely or on a local basis.
The filter is connected to the mains in a specified point of connection, thus guaranteeing a maximum level in the mains reactive current and/or in the total harmonic distortion flowing through the network.

Quantitative performance measures

The filter performance should be evaluated in a typical distribution system with different loads, linear and non-linear. The relevant performance indexes will be characterized by the total harmonic distortion (THD) of the mains current, with and without filter, in the following two indexes basis: filter effectiveness index and filter capacity index.
The Filtering Effectiveness index (FE) is the relation between the total harmonic distortion of the current supplied by the mains with and without filter in a pre-defined frequency range, according to some standard, e.g. EN 61000-3-2 or IEEE 519, (total harmonic cancellation results in a null factor):

$$FE = \frac{THD_{APF}}{THD} \tag{1}$$

The Filtering Capacity index (FC) is the relation between the total apparent power supplied by the filter and the total mains or load apparent power:

$$FC = \frac{S_{APF}}{S_{Load}} \tag{2}$$

These two indexes are the basis for evaluating the filter performance in static operation. In transient operation, only special conditions can be evaluated and they usually are not under the restrictions of power quality measurements, like those referred by the EN 50160 and the IEC 61000-4-30.

4. An APF example

Among the different alternatives, the direct current control strategy that generates the reference waveform for the AC source current was chosen for demonstration purposes (Chandra et al., 2000). It does not need to measure the load current or power, requires a low processing time and allows a fast calculation of the reference currents. The current-controlled pulse width modulation (PWM) with a medium frequency fixed carrier ensures enough bandwidth to implement the different active filtering goals.
To demonstrate these advantages, a three-phase 5 kVA prototype of an active filter is designed, and tested in dynamic and stationary operation with different load types.
The main block diagram of the system operation is shown in Fig. 3. It handles the two referred control strategies (Section 3.2) being capable of dealing with load harmonics elimination, power factor correction, load unbalancing compensation, and/or voltage regulation. The lower side generates the active current reference and the upper side the reactive component.
In this Chapter, it is implemented the first operating mode: power factor correction, harmonic elimination, and load unbalance compensation. So, the AC source power factor will be approximately one, and there is no need to control the voltage at the connection point.

The control algorithm needs the measurement of several variables like the three-phase AC source voltages and currents and the DC-link voltage. In a voltage distorted grid one of two compensating strategies can be chosen: 1- imposing sinusoidal currents in the grid or, 2- imposing unity power factor, (Cavallini & Montanari, 1994). However, the last strategy implies the circulation of harmonic currents in the grid; since medium voltage grids are usually very little distorted, it is not very used.

In a distorted grid and in order to impose sinusoidal currents in the source it is needed to low-pass filter the AC voltage, so obtaining the fundamental component. In an unbalanced grid it is needed to estimate the symmetrical components from the measured voltage signals. In this condition, the instantaneous positive sequence components can be obtained in the time domain with simple algebraic manipulation, (Hsu, 1998).

In steady-state, and neglecting losses in the active power filter, the active power supplied from the AC source should be equal to the demanded load active power, since no active power flows into the DC capacitor.

However, once the source voltage varies or the load power changes, the active power balance between the AC source and the load will not be maintained. This transient drives the average voltage of DC capacitor away from the reference voltage. So, in order to keep the active power filter operation, the amplitude of the grid current must be adjusted. The active power supplied from the source is then changed proportionally in order to compensate the active power supplied/received by the DC capacitor and match the active power consumed by the load. So, the AC source current amplitude can be obtained by regulating the DC capacitor voltage.

The active power balance in the DC-link determines the reference current of the AC source and the use of a PI controller allows a smooth control of the filter current and improves the system dynamic response. In this case, the schematic in Fig. 3 represents the essential block diagram of the current reference. The error in the DC voltage is transformed in active power to be controlled in the AC source.

4.1 Grid synchronization

With a three-phase balanced system or with the positive sequence component, the RMS voltage source amplitude, V_s, is calculated at the sampling frequency, f_s, from the source phase voltages, v_{sa}, v_{sb}, v_{sc}. At each sampling instant, it is expressed as in (3).

$$V_s = \sqrt{\frac{2}{3}(v_{sa}^2 + v_{sb}^2 + v_{sc}^2)} \tag{3}$$

The direct (or in-phase) unit current vectors are obtained from the AC source phase voltages and the RMS amplitude of the source voltage, V_s.

$$u_{si} = v_{si} / V_s; \qquad i = a,b,c \tag{4}$$

The unit current vectors implement one important function in the grid connection of a power electronics converter, the synchronization. This method is simple and robust and compares favourably with other methods like the decomposition of single-phase into orthogonal components method or the linear estimation of phase method, (Thomas & Woolfson, 2001).

4.2 Voltage controller

The AC source current has two active components: 1- the filter current, which maintains the DC bus voltage at a constant value and 2- the load current. So, all the filter losses, AC, DC and switching, are automatically compensated.

The reference stored energy on the DC-link capacitor is given by

$$E_{dcn} = \frac{1}{2} C V_{dcn}^2, \tag{5}$$

where V_{dcn} is the reference/nominal voltage across the capacitor, C.

When the capacitor is charged with a V_{dc} voltage the energy unbalance in the DC-link capacitor is

$$\Delta E_{dc} = \frac{1}{2} C (V_{dcn}^2 - V_{dc}^2) . \tag{6}$$

This energy unbalance must be supplied by the three-phase AC grid. Imposing a sinusoidal input current, the change in the capacitor energy must satisfy (7),

$$\Delta E_{dc} = \int_0^T \left[\sum_{i=0}^{2} V_m \sin(\omega_g t - \frac{2\pi}{3} i) I_{m1} \sin(\omega_g t - \frac{2\pi}{3} i) dt \right], \tag{7}$$

where I_{m1} is the active current supplied to the DC-link capacitor and ω_g is the grid angular frequency. So, the reference current to maintain the DC voltage is given by

$$I_{m1}^* = \frac{2}{3} \frac{\Delta E_{dc}}{T V_m} = C \frac{V_{dcn}^2 - V_{dc}^2}{3 T V_m}, \tag{8}$$

where T is the time interval where the averaging is calculated.

The total active component of the AC source current, I_s, is the sum of the filter current and the load current, I_l,

$$I_s = I_{m1} + I_l \tag{9}$$

However, the inclusion of the load current in the control algorithm implies additional current sensors and more signal processing to estimate the load active power, thus increasing the cost and decreasing the dynamic response, (Newman et al., 2002). A direct controller is then used; the voltage controller must directly provide the total active component of the AC source current.

The active component amplitude of the reference currents in the AC source, i_{sad}^* , i_{sbd}^* , i_{scd}^* , is calculated through a PI controller with anti-windup as shown in Fig. 4. The proportional and integral gains determine the controller behaviour in dynamic and static operation, (Newman et al., 2002, Marconi et al., 2007, Saetieo et al., 1995, Buso et al., 1998). As stated before, the correct active component, I_{sd}^* , of the AC source current is determined from the power balance in the DC-link. The current reference is then scaled with the unit current vectors in phase with the source voltage:

$$i_{si}^* = I_{sd}^* \cdot u_{si}; \quad i = a,b,c \tag{10}$$

4.3 Current controller

Hysteresis is the easiest control method to implement current control. One disadvantage is that it is difficult to limit the minimum and maximum switching frequencies in order to have a good tracking of the reference current.

Several solutions are known to overcome this limitation but they increase the controller complexity, (Zeng et al., 2004). Additionally, other features should be referred: 1- there is a lack of intercommunication between the individual hysteresis controllers and therefore no strategy to generate zero voltage vectors; 2- it has a tendency to lock into limit cycles of high frequency switching; and 3- it causes the generation of sub-harmonic current components, (Holmes & Lipo, 2003).

The direct current control method, in combination with a carrier-based pulse width modulation, gives a good performance at medium switching frequencies (in the range of 5 to 7 kHz). Its performance can only be degraded if used at low switching frequencies; this degradation is caused by the response time of the current controlled inverter, which leads to a phase shift between the reference currents and the output currents. So, the PWM-based current controller was selected for implementation.

In the modulation stage, shown in Fig. 5, the total reference currents are subtracted from the source current, thus obtaining a current error adapted according to the amplitude of the triangular carrier. Since the current error signal is always kept within the negative and positive peaks of the triangular waveform, the system has an inherent over current protection. The PWM output is completed with the introduction of an appropriate dead time in the control signals of the inverter transistors.

The filter output current is defined by the AC source voltage, the filter output voltage and the AC-link inductance.

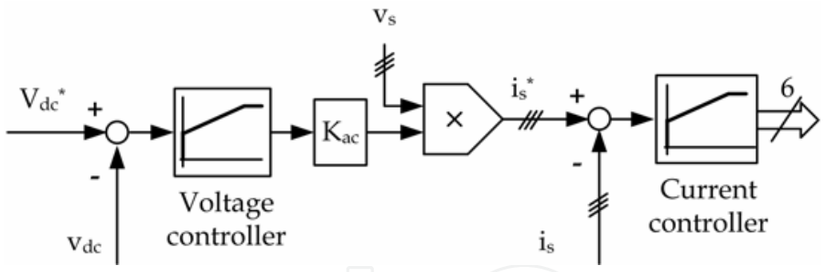

Fig. 4. Voltage and current controllers operation.

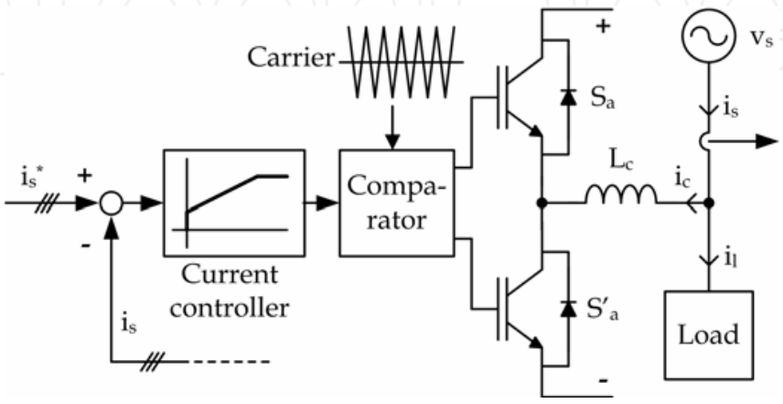

Fig. 5. Current control and PWM stage.

The current controller is designed according to the diagram in Fig. 6, where K_p and T_i are the PI controller gains, K_{inv} is the inverter gain and T_{inv} is the inverter time delay, equal to half of the switching period. Additionally, $T_L=L_c/R_c$ and $K_L=1/R_c$ and the measured current is filtered with a time constant T_f.

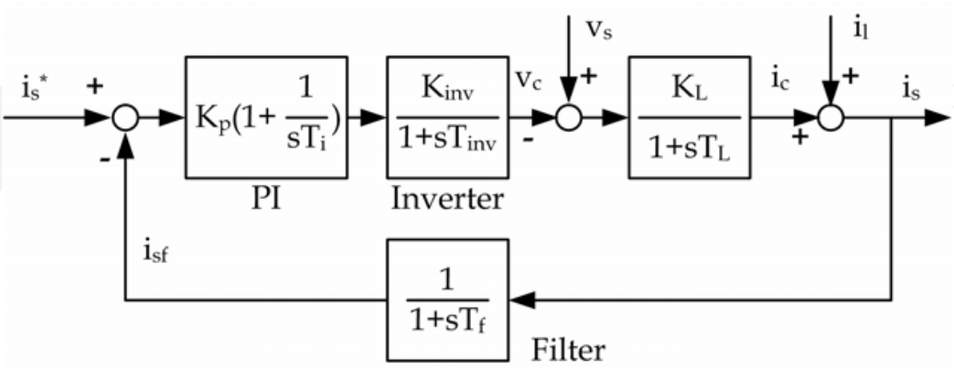

Fig. 6. Detailed model of the current control loop.

It is worthwhile to note that the closed loop transfer function is the same that is obtained with vector control; the only difference in the diagram of Fig. 6 is the absence of the cross term $\omega L_c i_{cq}$ in the voltage adding node, which is considered a disturbance.
The current controller open loop transfer function is

$$G_{oi}(s)=\frac{K_pK_{inv}K_L(1+sT_i)}{sT_i(1+sT_{inv})(1+sT_L)(1+sT_f)}. \tag{11}$$

Assuming that $T_i=T_L=L_c/R_c$, and that the two time constants, T_{inv} and T_f, can be approximated by one because they are quite small, the closed loop transfer function can be expressed as:

$$\frac{I_s}{I_s^*}=\frac{\omega_n^2}{s^2+2\xi\omega_n s+\omega_n^2}, \tag{12}$$

with

$$\xi=\frac{1}{2}\sqrt{\frac{1}{KT_{sf}}};\quad \omega_n=\sqrt{\frac{K}{T_{sf}}} \tag{13}$$

In (13) the two constants are given by:

$$T_{sf}=T_{inv}+T_f;\quad K=\frac{K_pK_{inv}K_L}{T_i}. \tag{14}$$

According to the assumption made, $T_i=T_L$, the parameter K_p determines the damping factor of the control loop and, simultaneously, the speed response. Thus, knowing the filter parameters and imposing the dynamic behaviour the current controller gains can be obtained.

5. Inductive and capacitive components

The selection of the AC-link inductance and the DC-link capacitor values affects directly the performance of the active power filter. Static VAR compensators and active filters implemented with voltage-source inverters present the same power topology, but the criteria used to select the values of L and C are different. The active filter can implement the two compensation modes simultaneously, so it is presented the two main design criteria to accomplish these objectives: fundamental component reactive power compensation and harmonics compensation.

5.1 Inductive filter design

One possibility to design the inductance is to consider the maximum current, I_{max}, that the filter must supply in order to compensate a totally inductive load. In this condition the inductance and the inverter must be dimensioned taking into consideration the apparent power to be compensated. A simple phasor diagram analysis, shown in Fig. 7, gives the inductance value as in (15):

$$L_{\min} = \frac{\Delta V_{\min}}{\omega_g I_{\max}} \tag{15}$$

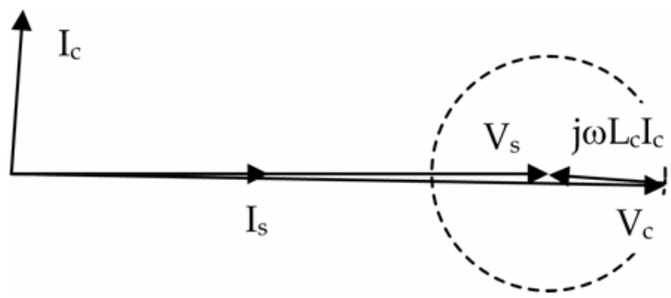

Fig. 7. Maximum output filter voltage with reactive power compensation.

ΔV_{min} is the difference between the RMS source voltage and the fundamental component RMS inverter voltage, which depends on the values of the DC-link voltage and the modulation index, and ω_g is the value of the grid frequency. If the inductive voltage drop, ΔV, is made small the inductance will be small and there is a better utilization of the DC voltage. However, a very small inductance implies a high voltage gain and introduces a higher complexity in the controller design. Additionally, the ripple current will increase. In order to keep the ripple current at a reduced level, the inductive voltage drop should be kept at a minimum value.

As an active filter, the inductance value should be decreased to be capable of higher surge currents and harmonic currents. In this condition, another criterion can be evaluated, like the one referred in Moran et al. (1995). Imposing a fixed switching frequency, f_s, and the maximum di/dt of the current to be compensated, the inductance value is now given by:

$$L_{\max} = \frac{\Delta V_{\max}}{4\left(di/dt\right)_{\max} \cdot f_s} \tag{16}$$

ΔV_{max} is the maximum difference between the instantaneous AC source voltage and the instantaneous inverter voltage. From this point of view a higher DC-link voltage allows a higher di/dt, so increasing the active filter frequency response.
If the ripple current can be reduced through an increasing in the switching frequency or an increasing in the controller dynamics the inductance value would not be so influent in the global filter performance. The connecting inductances also decouple the output inverter voltage from the AC source voltage.
Considering, designing, and ranking all the referred factors, including the filter compensation modes, an indicative value for the inductance can be obtained.

5.2 DC-link capacitor design

The DC-link capacitor can be designed according to distinct objectives, the most important one being keeping the DC-link voltage fluctuation limited. The reactive power supplied by the filter corresponds to a stored energy in the AC inductors. When a reactive power compensation change is demanded, there occurs a variation in the stored energy associated with the final and initial values of the filter reactive current, I_1 and I_0, respectively:

$$\Delta E = \frac{3}{2} L(I_0^2 - I_1^2) . \tag{17}$$

In the worst case of a totally inductive to totally capacitive compensation change, it can be assumed that the energy change in the inductors has to be supplied by the DC-link capacitor. So, the DC voltage fluctuates in transient operation, according to supplying or absorbing the energy; the DC-link capacitor has to be designed to moderate the DC voltage fluctuation.
When the DC voltage changes from V_{dc0} to V_{dc1}, the energy released from the DC-link capacitor, is given by (18) if it is assumed a small change in V_{dc}.

$$\Delta E_{dc} = \frac{1}{2} C(V_{dc0}^2 - V_{dc1}^2) \cong C V_{dc0}(V_{dc0} - V_{dc1}) , \tag{18}$$

Introducing the ratio of the DC voltage change, ε, defined by

$$\varepsilon = \frac{V_{dc0} - V_{dc1}}{V_{dc0}} = \frac{\Delta V_{dc}}{V_{dc0}} , \tag{19}$$

the required DC capacitor is given by

$$C = \frac{3L(I_0^2 - I_1^2)}{2\varepsilon V_{dc0}^2} . \tag{20}$$

Analysis of (20) shows that the required capacitance of the DC capacitor is proportional to the line inductance and inversely proportional to the specified DC voltage fluctuation. The value of the DC-link capacitor can also be designed in order to supply active power to the load during a pre-defined time interval in case of AC source absence.
Thus, knowing the AC connecting inductance, the nominal DC voltage and the allowed voltage fluctuation, the DC capacitor value can be obtained.

6. Simulation and experimental results

The Saber Designer software package was used to design, simulate, and test the active filter control algorithm. In order to implement the algorithm in digital hardware platform it was built a simulation model of a microcontroller. So, the C code written and validated in the Saber environment can be easily transferred to any hardware target.

6.1 Simulation results

Different active filtering conditions, power factor compensation, and load balancing tests have been done, in transient and static operation and for linear and non-linear loads. The transient operation tests were made putting the active filter into operation when the load was already connected to the AC source voltage and also with simultaneous connection of both, load and filter.

In Fig. 8 the non-linear load is a three-phase diode rectifier, with a DC current of 7 A and a DC voltage of 250 V. [The other filter parameters are given in Table 1.] The transient operation test was made first connecting the filter and then connecting the load under test.

Nominal power	5 kVA
Supply voltage	110/190 V, 50 Hz
DC voltage	350 V, DC capacitor: 1.6 mF
Switching frequency	5 kHz, dead time: 4 μs
Filter inductance	L_c, R_c: 2 mH, 0.2 Ω
DC voltage controller	K_{pv}, T_{iv}: 0.01, 100 ms
Current controller	K_{ip}, T_{ii}: 0.007, 10 ms

Table 1. System parameters (simulation and experimental).

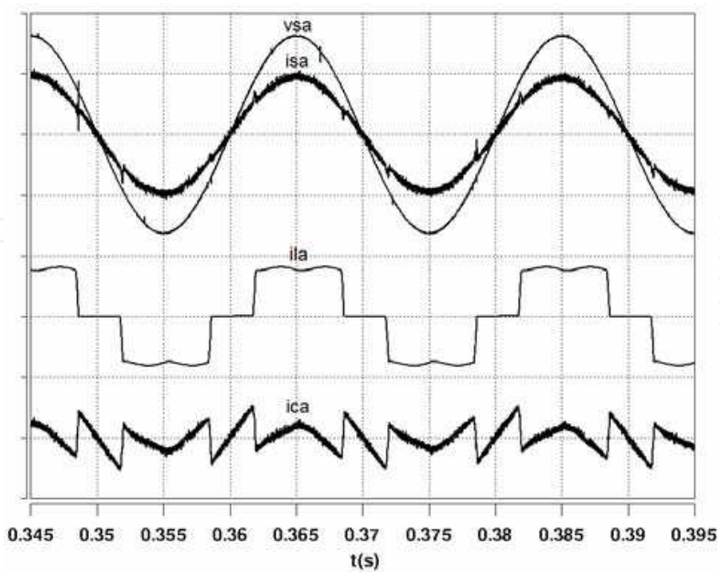

Fig. 8. Steady-state compensation of a three-phase diode rectifier. Traces from top to bottom (phase a): source voltage, v_{sa}, (100 V/div); source current, i_{sa}, (10 A/div); load current, i_{la}, (10 A/div); filter current, i_{ca}, (10 A/div).

As can be seen, except for the high di/dt intervals, the active filter completely compensates the rectifier harmonic currents. A smaller inductance would produce a better low-frequency compensation but with high ripple current. The APF performance is demonstrated in Fig. 9, showing the harmonic distortion of the source current with and without filter.

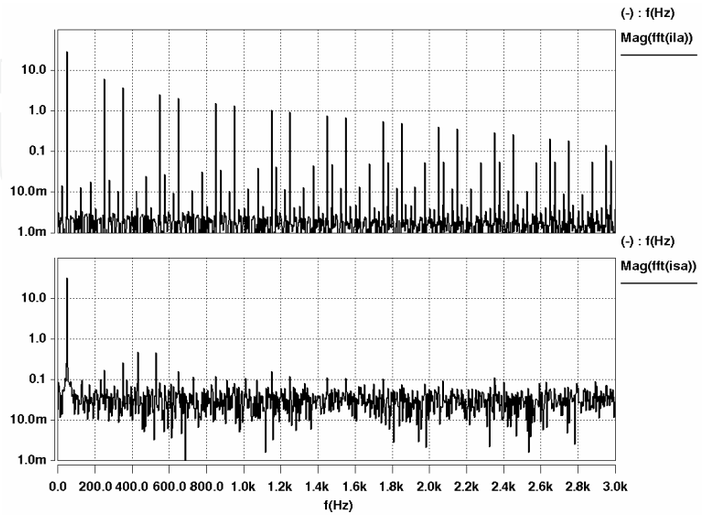

Fig. 9. Harmonic spectrum of phase a non-linear load current (top) and AC source current (bottom), with the APF connected, corresponding to Fig. 8.

Transient operation with the same load is shown in Fig. 10. It can be noticed a short interval where the AC source current is out of phase with the voltage but it quickly gets in phase.

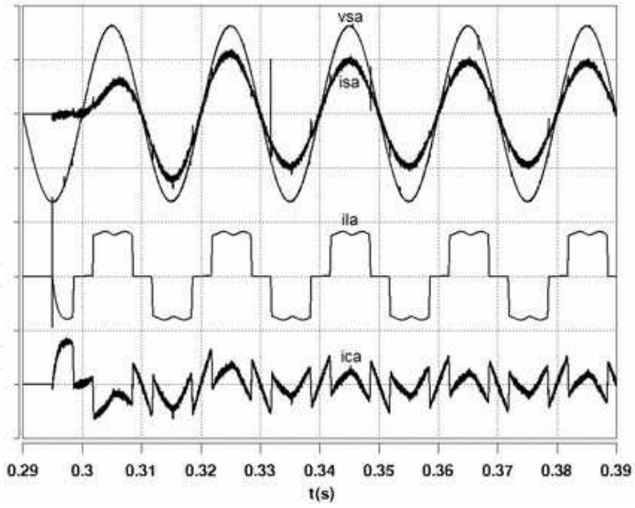

Fig. 10. Transient compensation of a three-phase diode rectifier; filter connected before the load. Traces from top to bottom (phase a): source voltage, v_{sa}, (100 V/div); source current, i_{sa}, (10 A/div); load current, i_{la}, (10 A/div); filter current, i_{ca}, (10 A/div).

The same non-linear load type, but now a three-phase thyristor bridge was used to perform the test shown in Fig. 11. The bridge firing angle is 30^{o}, thus generating not only low-frequency harmonics but also a reactive current component at fundamental frequency. Fig.

11 shows the same waveforms already presented in Fig. 8, and Fig. 12 shows the source current spectrum without and with compensation. Differently from Fig. 10, Fig. 13 shows the transient response when the filter is connected to the system with the non-linear load already supplied by the source voltage.

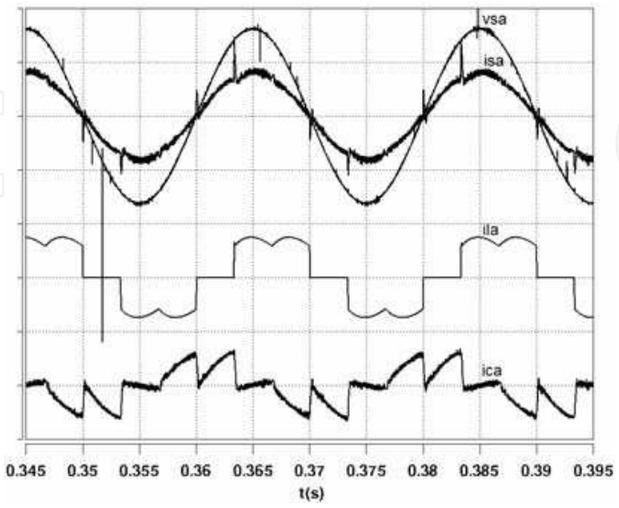

Fig. 11. Steady-state compensation of a three-phase thyristor rectifier, with a firing angle of 30°. Traces from top to bottom (phase a): source voltage, v_{sa}, (100 V/div); source current, i_{sa}, (10 A/div); load current, i_{la}, (10 A/div); filter current, i_{ca}, (10 A/div).

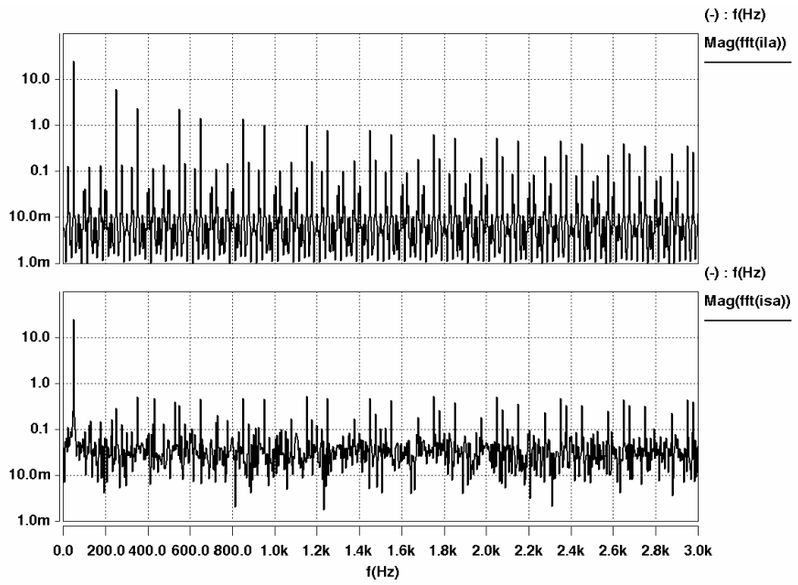

Fig. 12. Harmonic spectrum of phase a non-linear load current (top) and AC source current (bottom), with the APF connected, corresponding to Fig. 11.

The simulation of the filter operation in load unbalance compensation is shown in two conditions, with linear (Fig. 14) and non-linear load (Fig. 15). In Fig. 14, a linear load is connected between phases a and b, leaving phase c in open circuit.

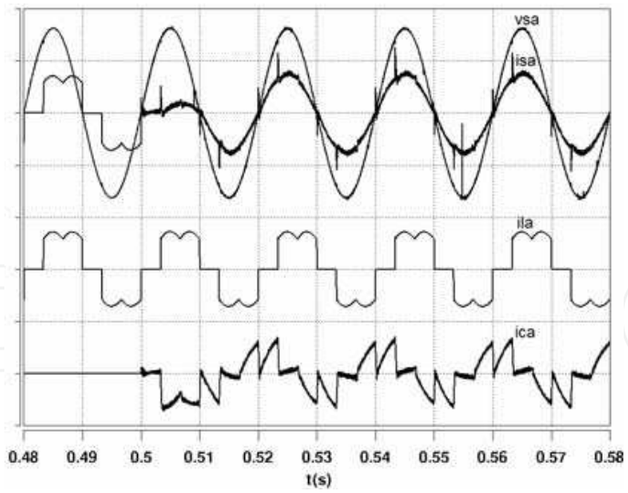

Fig. 13. Transient compensation of a three-phase thyristor rectifier, with a firing angle of 30°; filter connected after the load. Traces from top to bottom (phase a): source voltage, v_{sa}, (100 V/div); source current, i_{sa}, (10 A/div); load current, i_{la}, (10 A/div); filter current, i_{ca}, (10/div).

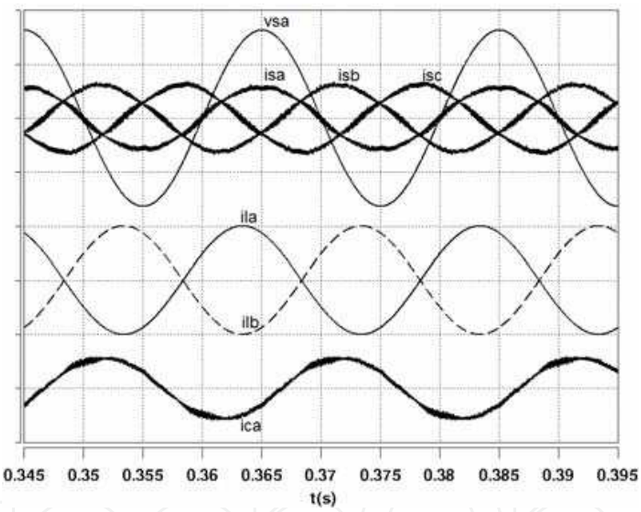

Fig. 14. Load unbalance compensation with linear load. Traces from top to bottom: source voltage (phase a), v_{sa}, (100 V/div); source currents, i_{sa}, i_{sb}, i_{sc}, (10 A/div); load currents, i_{la}, i_{lb}, (10 A/div); filter current, i_{ca}, (10 A/div).

In Fig. 15, the load is a single-phase diode rectifier bridge, connected between two phases (a and b); the third phase is opened. In either condition the unbalance compensation is not perfect, as can be also concluded from Fig. 16, which shows the spectrum of phase a source current. It should be referred the effect of the small DC voltage fluctuation and the effect of the relatively high value of the AC inductance.

If the unbalanced load is the condition that would be the most important in the filter operation then the DC-link capacitor value could be increased. Also, the AC inductance value can be decreased but the switching frequency must rise to keep the high order harmonics at low levels. Alternatively, small passive filters can be used at the point of common coupling.

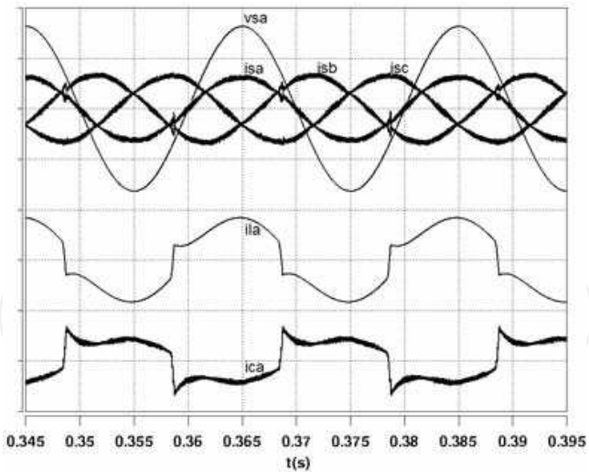

Fig. 15. Load unbalance compensation (non-linear load). Traces from top to bottom: phase a source voltage, v_{sa}, (100 V/div); source currents, i_{sa}, i_{sb}, i_{sc}, (10 A/div); load current, i_{la}, (10 A/div); filter current, i_{ca}, (10 A/div).

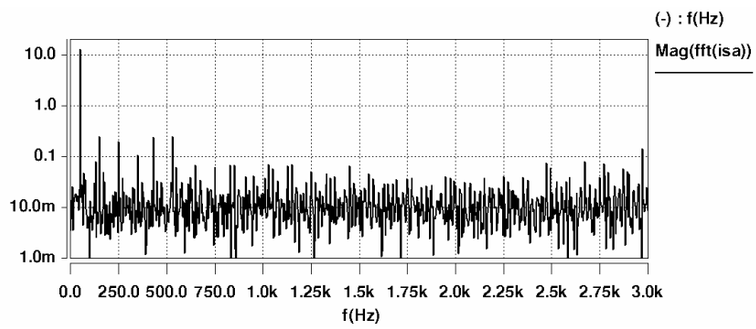

Fig. 16. Harmonic spectrum of the balanced AC source current (Fig. 15) originated from a non-linear and unbalanced load current.

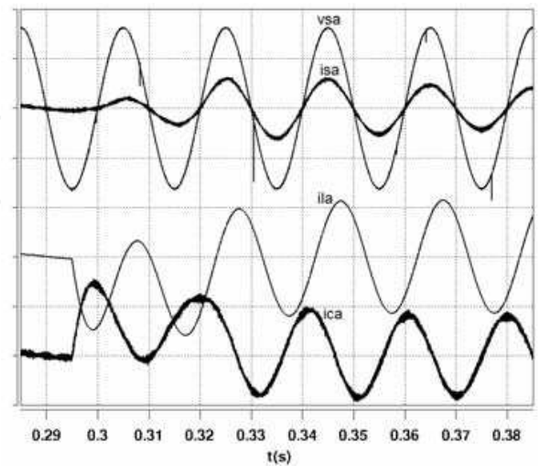

Fig. 17. No-load induction motor magnetization. Traces from top to bottom (phase a): source voltage, v_{sa}, (100 V/div); source current, i_{sa}, (20 A/div); load current, i_{la}, (10 A/div); filter current, i_{ca}, (10 A/div).

Finally, Fig. 17 shows the simulation of the filter operation when an induction motor is directly connected to the source in free acceleration mode and no mechanical load. In this case, it can be observed a DC transient in the motor current, quickly compensated by the filter as can be verified in the source current.
The conclusion from the presented simulation results is that the control algorithm succeeded in the most important functions of the active power filter, harmonics mitigation, reactive power compensation and load unbalance compensation.

6.2 Experimental results

An experimental three-phase active filter prototype has been designed for a nominal power of 5 kVA. It is based on a voltage source inverter with MOSFET transistors and a switching frequency of 5 kHz. The control platform is build over a TERN 586-Engine, a module with a C++ programmable microprocessor, with a 32-bit CPU operating at 100 MHz that includes a math coprocessor for floating point operations. Several I/O interfaces are available, including 8 channel, 12-bit A/D converter; series D/A converter; 32 I/O lines; 15 external interrupts, and seven 16-bit timers.
Similar experimental tests have been conducted and the results can be viewed in two perspectives: validation of the global simulation model, and measure of the active filter performance. The experimental tests were conducted in a laboratory with an important distortion in the mains voltage, due to the proximity of a large number of non-linear loads. However, the mains current waveform after compensation is almost a sine wave due to the extraction of the fundamental component of the mains voltage through low-pass filters. This filter action allows the imposition of sine wave references for the source current; it could be possible to impose non-sine wave references "in phase" with the mains voltage, (Cavallini & Montanari, 1994).
The non-linear load present in Fig. 18 and Fig. 19 is a three-phase diode rectifier. In Fig. 18 it can be seen the steady-state compensation, where the AC source current gets a sine wave form, being only slightly distorted in the instants of the diode switching. This is due to the high di/dt occurring in these points, which is impossible to compensate unless with a very high DC voltage or a very low AC inductance. There should be a compromise between the active filter dimensioning and the characteristics of the load current to be compensated. Fig. 19 shows the filter transient operation with the same load condition.

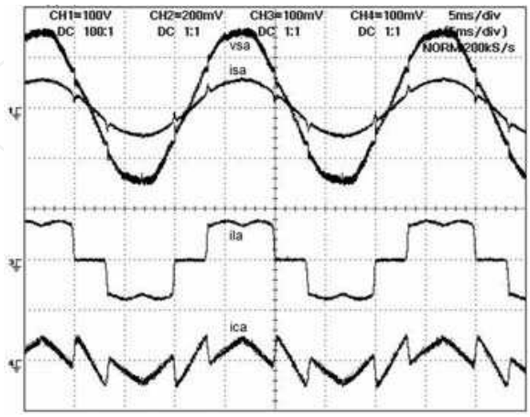

Fig. 18. Steady-state compensation of a three-phase diode rectifier. Traces from top to bottom (phase a): source voltage, v_{sa}, (100 V/div); source current, i_{sa}, (20 A/div); load current, i_{la}, (10 A/div); filter current, i_{ca}, (10 A/div).

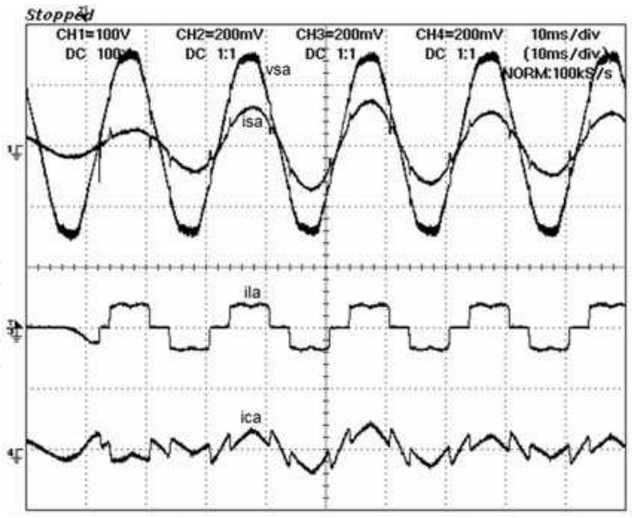

Fig. 19. Transient compensation of a three-phase diode rectifier. Traces from top to bottom (phase a): source voltage, v_{sa}, (100 V/div); source current, i_{sa}, (20 A/div); load current, i_{la}, (20 A/div); filter current, i_{ca}, (20 A/div).

In Fig. 20 it is presented the balancing action of the active filter compensating an unbalanced load (a single-phase diode rectifier bridge, connected between two phases; the third phase is an open circuit).

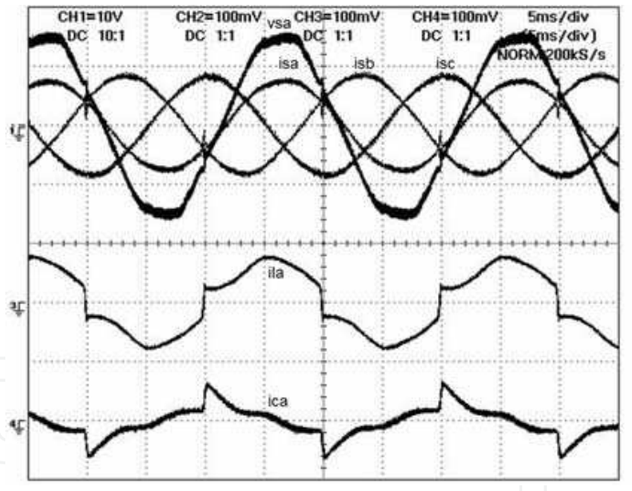

Fig. 20. Load unbalance compensation. Traces from top to bottom: source voltage (phase a), v_{sa}, (100 V/div); source currents, i_{sa}, i_{sb}, i_{sc}, (10 A/div); load current, i_{la}, (10 A/div); filter current, i_{ca}, (10 A/div).

In Fig. 21 it can be seen the active filter behaviour in a no-load induction motor magnetization. The filter quickly compensates the load power factor and the decaying DC component. In this case, the transient response is also dependent on the time interval where the load current has a non-zero DC value.

As expected, the experimental results are in close agreement with the simulation ones thus validating the control algorithm as in its operating principle as in its digital implementation.

6.3 Discussion

Four simulated results can be compared with the experimental ones. Figures 8 and 18 show the steady-state operation with the filter compensating a typical non-linear load, and close agreement between the two can be noticed even with a distorted grid in the lab.

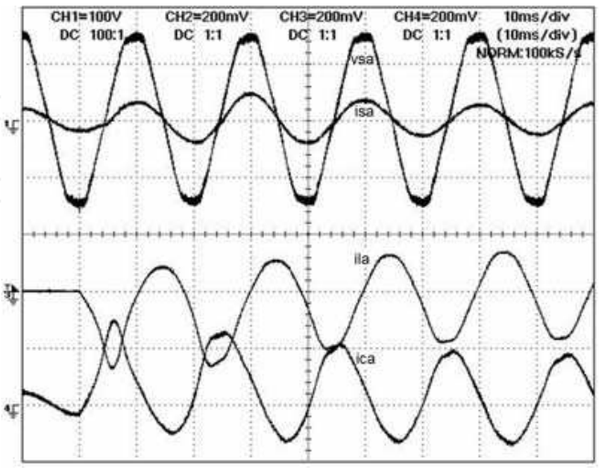

Fig. 21. No-load induction motor magnetization. Traces from top to bottom (phase a): source voltage, v_{sa}, (100 V/div); source current, i_{sa}, (20 A/div); load current, i_{la}, (10 A/div); filter current, i_{ca}, (10 A/div).

Figures 10 and 19, related to the transient operation with the same non-linear load, show very similar results; the filter operating principle, based on energy balance between AC inductance and DC capacitor, is validated.

Load balancing, analyzed in Figures 15 and 20, is an easy task with this control method. It is automatically achieved; it does not need decomposition of the load current into symmetrical components.

Figures 17 and 21 demonstrate an additional benefit of the active power filter: minimization of DC transients. This is an important feature especially in weak grids where long DC current transients cause also DC transients in the AC voltage, particularly harmful for transformers and electric machines.

7. Conclusions and further research

7.1 Conclusions

An active power filter is a high performance power electronics converter and can operate in different modes: harmonics elimination, power factor correction, voltage regulation and load unbalance compensation. Different control approaches are possible but they all share a common objective: imposing sinusoidal currents in the grid, eventually with unity power factor, even in the case of highly distorted mains voltage. This Chapter analyzes and compares different approaches to be used in the control of the APF.

As a demonstration of the capabilities of the APF, one control approach has been selected. It uses a simple and robust power circuit interface without load current sensors and an efficient signal processing without heavy or complex computations. Simulation results under different operating conditions demonstrate the overall possibilities of the control method and of the active power filter globally.

Also, the presented experimental implementation has been validated and can be applied in different operating modes: harmonics active filtering, power factor correction, and balancing of linear or non-linear loads, single or grouped, which cause great perturbation and performance degradation in the power quality of an electrical distribution system.

7.2 Further research

Active power filters are now well established in the market. However, some issues still need further research. The filter dynamics depends on the switching frequency; higher frequencies given better results but also higher losses. Specific modulation strategies and control algorithms must be improved. In particular selective harmonic elimination methods can bring additional performance. Also, multilevel based topologies allow the APF to reach higher voltages and power and so give the filter the possibility of being applied in the power systems domain.

8. References

Akagi, H., Kanazawa, Y. & Nabae, A. (1984). Instantaneous reactive power compensators comprising switching devices without energy storage components. *IEEE Transactions on Industry Applications*, vol. 20, nº 3, (May/June 1984), pp. 625-630, ISSN 0093-9994.

Akagi, H. (2005). Active harmonic filters. *Proceedings of the IEEE*, vol. 93, nº 12, (Dec. 2005), pp. 2128-2141, ISSN 0018-9219.

Akagi, H., Watanabe, E.H. & Aredes, M. (2007). *Instantaneous Power Theory and Applications to Power Conditioning*. IEEE Press, ISBN 978-0-470-10761-4, Piscataway, New Jersey.

Aredes, M., Hafner, J. & Heumann, K. (1997). Three-phase four-wire shunt active filter control strategies. *IEEE Transactions on Power Electronics*, vol. 12, nº 2, (March 1997), pp. 311-318, ISSN 0885-8993.

Bhattacharya, S., Veltman, A., Divan, D.M. & Lorenz, R.D. (1996). Flux-based active filter controller. *IEEE Transactions on Industry Applications*, vol. 32, nº 3, (May/June 1996), pp. 491-502, ISSN 0093-9994.

Bollen, M.H. (1999). *Understanding Power Quality Problems: Voltage Sags and Interruptions*. Wiley-IEEE Press, ISBN 0-7803-4713-7, Piscataway, New Jersey.

Buso, S., Malesani, L. & Mattavelli P. (1998). Comparison of current control techniques for active filter applications. *IEEE Transactions on Industrial Electronics*, vol. 45, nº 5, (Oct. 1998), pp. 722-729, ISSN 0278-0046.

Cavallini, A. & Montanari, G.R. (1994). Compensation strategies for shunt active filter control. *IEEE Transactions on Power Electronics*, vol. 9, nº 6, (Nov. 1994), pp. 587-593, ISSN 0885-8993.

Chandra, A., Singh, B., Singh, B.N., Al-Haddad, K. (2000). An improved control algorithm of shunt active filter for voltage regulation, harmonic elimination, power factor correction and balancing of nonlinear loads. *IEEE Transactions on Power Electronics*, vol. 15, nº 3, (May/Jun. 2000), pp. 495-507, ISSN 0885-8993.

Chen, B.S., & Joós, G. (2008). Direct power control of active filters with averaged switching frequency regulation. *IEEE Transactions on Power Electronics*, vol. 23, nº 6, (Nov. 2008), pp. 2729-2737, ISSN 0885-8993.

Chen, C.L., Lin, C.E. & Huang, C.L. (1993). Reactive and harmonic current compensation for unbalanced three-phase systems using the synchronous detection method. *Electric Power Systems Research*, vol. 26, nº 3, (Apr. 1993), pp. 163-170, ISSN 0378-7796.

Furuhashi, T., Okuma, S. & Uchikawa, Y. (1990). A study on the theory of instantaneous reactive power. *IEEE Transactions on Industrial Electronics*, vol. 37, nº 1, (Jan./Feb. 1990), pp. 86-90, ISSN 0278-0046.

Hingorani, N.G. & Gyugyi, L. (1999). *Understanding Facts: Concepts and Technology of Flexible AC Transmission Systems*. Wiley-IEEE Press, ISBN 0-7803-3455-8, Piscataway, New Jersey.

Holmes, D.G. & Lipo, T.A. (2003). *Pulse Width Modulation for Power Converters. Principles and Practice*. IEEE Press, ISBN 0-471-20814-0, Piscataway, New Jersey.

Hsu, J.S. (1998). Instantaneous phasor method for obtaining instantaneous balanced fundamental components for power quality control and continuous diagnostics. *IEEE Transactions on Power Delivery*, vol. 13, nº 4, (Oct. 1998), pp. 1494-1500, ISSN 0885-8977.

Komurcugil, H. & Kukrer, O. (2006). A new control strategy for single-phase shunt active power filters using a Lyapunov function. *IEEE Transactions on Industrial Electronics*, vol. 53, nº 1, (Feb. 2006), pp. 305-312, ISSN 0278-0046.

Lascu, C., Asiminoaei, L., Boldea, I. & Blaabjerg, F. (2007). High performance current controller for selective harmonic compensation in active power filters. *IEEE Transactions on Power Electronics*, vol. 22, nº 5, (Sept. 2007), pp. 1826-1835, ISSN 0885-8993.

Lin, B.-R. & Yang, T.-Y. (2004). Three-level voltage-source inverter for shunt active filter. *IEE Proceedings Electric Power Applications*, vol. 151, nº 6, (Nov. 2004), pp. 744-751, ISSN 1350-2352.

Marconi, L., Ronchi, F. & Tilli, A. (2007). Robust nonlinear control of shunt active filters for harmonic current compensation. *Automatica*, vol. 43, nº2, (Feb. 2007), pp. 252-263, ISSN 0005-1098.

Mendalek, N., Al-Haddad, K., Fnaiech, F. & Dessaint, L.A. (2003). Nonlinear control technique to enhance dynamic performance of a shunt active power filter. *IEE Proceedings Electric Power Applications*, vol. 150, nº 4, (July 2003), pp. 373-379, ISSN 1350-2352.

Montero, M.I.M., Cadaval, E.R. & González, F.B. (2007). Comparison of control strategies for shunt active power filters in three-phase four-wire systems. *IEEE Transactions on Power Electronics*, vol. 22, nº 1, (Jan. 2007), pp. 229-236, ISSN 0885-8993.

Morán, L.A., Dixon, J.W. & Wallace, R.R. (1995). A three-phase active power filter operating with fixed switching frequency for reactive power and current harmonic compensation. *IEEE Transactions on Industrial Electronics*, vol. 42, nº 4, (Aug. 1995), pp. 402-408, ISSN 0278-0046.

Newman, M.J., Zmood, D.N. & Holmes, D.G. (2002). Stationary frame harmonic reference generation for active filter systems. *IEEE Transactions on Industry Applications*. vol. 38, nº 6, (Nov./Dec. 2002), pp. 1591-1599, ISSN 0093-9994.

Routimo, M., Salo, M. & Tuusa, H. (2007). Comparison of voltage-source and current-source shunt active power filters. *IEEE Transactions on Power Electronics*, vol. 22, nº 2, (March 2007), pp. 636-643, ISSN 0885-8993.

Saetieo, S., Devaraj, R. & Torrey, D.A. (1995). The design and implementation of a three-phase active power filter based on sliding mode control. *IEEE Transactions on Industry Applications*, vol. 31, nº 5, (Sept./Oct. 1995), pp. 993-1000, ISSN 0093-9994.

Thomas, D.W.P. & Woolfson, M.S., (2001). Evaluation of frequency tracking methods. *IEEE Transactions on Power Delivery*, vol. 16, nº 3, (July 2001), pp. 367-371, ISSN 0885-8977.

Zeng, J., Yu, C., Qi, Q., Yan, Z., Ni, Y., Zhang, B.L., Chen, S. & Wu, F.F. (2004). A novel hysteresis current control for active power filter with constant frequency. *Electric Power Systems Research*, vol. 68, (2004), pp. 75-82, ISSN 0378-7796.

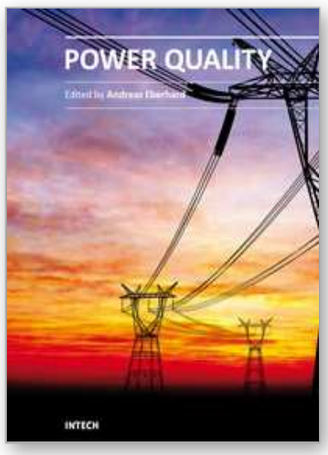

Power Quality

Edited by Mr Andreas Eberhard

ISBN 978-953-307-180-0
Hard cover, 362 pages
Publisher InTech
Published online 11, April, 2011
Published in print edition April, 2011

Almost all experts are in agreement - although we will see an improvement in metering and control of the power flow, Power Quality will suffer. This book will give an overview of how power quality might impact our lives today and tomorrow, introduce new ways to monitor power quality and inform us about interesting possibilities to mitigate power quality problems.

How to reference

In order to correctly reference this scholarly work, feel free to copy and paste the following:

António Martins, José Ferreira and Helder Azevedo (2011). Active Power Filters for Harmonic Elimination and Power Quality Improvement, Power Quality, Mr Andreas Eberhard (Ed.), ISBN: 978-953-307-180-0, InTech, Available from: http://www.intechopen.com/books/power-quality/active-power-filters-for-harmonic-elimination-and-power-quality-improvement

INTECH
open science | open minds

InTech Europe
University Campus STeP Ri
Slavka Krautzeka 83/A
51000 Rijeka, Croatia
Phone: +385 (51) 770 447
Fax: +385 (51) 686 166
www.intechopen.com

InTech China
Unit 405, Office Block, Hotel Equatorial Shanghai
No.65, Yan An Road (West), Shanghai, 200040, China
中国上海市延安西路65号上海国际贵都大饭店办公楼405单元
Phone: +86-21-62489820
Fax: +86-21-62489821

IntechOpen